

# Outline of Contents

	<b>Pages</b>
Acknowledgments	
Outline of Contents	I
List of Tables	VIII
List of Figures	X
Abstract (in Chinese)	XIV
Abstract (in English)	XVI
<b>Chapter 1 Introduction</b>	
1.1 Overview on Benzoxazines and Polybenzoxazines (PBZZs)	1
1.1.1 Syntheses of Benzoxazines and Thermal Curing of Polybenzoxazines	1
1.1.2 Features of Polybenzoxazines	3
1.2 Polymer and Miscibility and Interactions	4
1.3 Reference Review	6
1.3.1 Syntheses of various Benzoxazines and Polybenzoxazines	6
1.3.2 Polymer Blending of Polybenzoxazines	7
References	10
<b>Chapter 2</b>	
2.1 Overview on Low Dielectric Constant Materials for IC Applications	12
2.1.1 Requirements for interlayer and intermetal dielectrics	14
2.1.2 Dielectric Constant and Bonding Characteristics	16
2.1.3 Porous Low Dielectric Materials	17
2.2 Overview on Cyclodextrins	18
2.2.1 Structural Features of Cyclodextrins	18
2.2.2 CD Inclusion Complexes	22

2.2.3 Two Types of Crystal Structures: Channel-type and Cage-type	24
2.2.4 Rotaxanes and Pseudorotaxanes	26
2.3 Reference Review	28
2.3.1. Low Dielectric Constant Materials	28
2.3.2 Complex Formation of Cyclodextrins with Hydrophilic Polymers	29
References	32

### Chapter 3 Thermal Properties and Hydrogen Bonding in Polymer Blend of Polybenzoxazine/Poly (N-vinyl-2-pyrrolidone)

Abstract

3.1 Introduction	37
3.2 Experimental	
3.2.1 Materials	38
3.2.2 Blend Preparations	38
3.2.3 Differential Scanning Calorimetry (DSC)	39
3.2.4 Infrared Spectroscopy	39
3.3 Results and Discussion	
3.3.1 Glass Transition Temperature Analysis	40
3.3.2 Fourier Transfer Infrared Spectroscopy Analysis	41
3.3.3 The Self-Association of Hydroxyl Groups of PBZZ	42
3.3.4 The Equilibrium Constants of Inter-Association	44
3.4 Conclusions	46
References	47

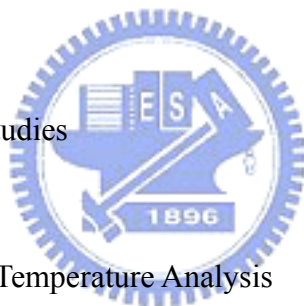


### Chapter 4 The Kinetics of B-a and P-a Type Copolybenzoxazine via Ring Opening

## Process

### Abstract

4.1	Introduction	62
4.2	Experimental	
4.2.1	Materials	62
4.2.2	Reactants Preparations	63
4.2.3	Differential Scanning Calorimetry (DSC)	63
4.2.4	Isothermal Curing	63
4.2.5	Dynamic Curing	63
4.2.6	Glass Transition Temperatures Measurement	64
4.2.7	Infrared Spectroscopy	64
4.3	Results and Discussion	
4.3.1	Scanning DSC Studies	65
4.3.2	Kinetic Analysis	66
4.3.3	Glass Transition Temperature Analysis	69
4.3.4	Fourier Transfer Infrared Spectroscopy Analysis	69
4.4	Conclusions	71
	References	72

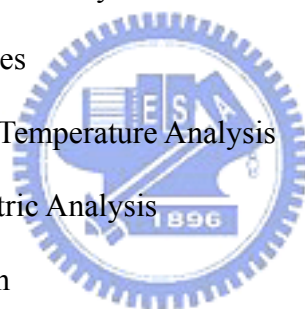


## Chapter 5 Synthesis and Characterization of Fluorinated Polybenzoxazine Material with Low Dielectric Constant

### Abstract

5.1	Introduction	81
5.2	Experimental	
5.2.1	Synthesis of F-1 benzoxazine	87

5.2.2 Nuclear Magnetic Resonance (NMR)	87
5.2.3 Fourier Transform Infrared Spectroscopy (FT-IR)	87
5.2.4 Reactants Preparations	88
5.2.5 Dielectric Analysis	88
5.2.6 Differential Scanning Calorimetry (DSC)	88
5.2.7 Thermogravimetric Analysis (TGA)	89
5.2.8 Water Absorption	89
5.3 Results and Discussion	
5.3.1 Nuclear Magnetic Resonance Analysis	90
5.3.2 Fourier Transfer Infrared Spectroscopy Analysis	90
5.3.3 Dielectric Constant Analysis	91
5.3.4 Thermal Properties	92
5.3.5 Glass Transition Temperature Analysis	92
5.3.6 Thermogravimetric Analysis	94
5.3.7 Water Absorption	94
5.4 Conclusions	96
References	97



## Chapter 6 Study of the Morphologies and Dielectric Constants of Nanoporous

Materials Derived from Benzoxazine-Terminated Poly( $\epsilon$ -caprolactone)/

Polybenzoxazine Copolymers

Abstract

6.1 Introduction	109
6.2 Experimental	

6.2.1 Materials	111
6.2.2 Synthesis of pa-OH	112
6.2.3 Syntheses of pa-OH terminated PCL (pa-PCL)	113
6.2.4 Preparation of Reactants	113
6.2.5 Nuclear Magnetic Resonance (NMR)	114
6.2.6 Fourier Transform Infrared Spectroscopy (FT-IR)	114
6.2.7 Differential Scanning Calorimetry (DSC)	114
6.2.8 Thermogravimetric Analysis (TGA)	115
6.2.9 Field Emission Scanning Electron Microscopy (FE-SEM)	115
6.2.10 Dielectric Analysis	116
6.3 Results and Discussion	
6.3.1 Nuclear Magnetic Resonance Analyses	117
6.3.2 Fourier Transfer Infrared Spectroscopy Analyses	117
6.3.3 Differential Scanning Calorimetry Analyses	118
6.3.4 Thermogravimertric Analyses	120
6.3.5 Scanning Electron Microscopy Analysis	121
6.3.6 Dielectric Analysis	122
6.4 Conclusions	124
References	125

## Chapter 7 Synthesis and Characterization of Novel Adamantane-Modified

### Polybenzoxazine

#### Abstract

7.1 Introduction	141
7.2 Experimental	


7.2.1	Materials	142
7.2.2	Synthesis of 4-(1-Adamantyl)phenol	142
7.2.3	Synthesis of 6-adamantyl-3-phenyl-3,4-dihydro-2H-1,3-benzoxazine	143
7.2.4	Synthesis of 6-adamantyl-3-methyl-3,4-dihydro-2H-1,3-benzoxazine	143
7.2.5	Nuclear Magnetic Resonance (NMR)	143
7.2.6	Differential Scanning Calorimetry (DSC)	144
7.2.7	Thermogravimetric Analysis (TGA)	144
7.3	Results and Discussion	
7.3.1	Nuclear Magnetic Resonance Analyses	145
7.3.2	Fourier Transfer Infrared Spectroscopy Analysis	145
7.3.3	Glass Transition Temperature Analyses	146
7.3.4	Thermogravimetric Analyses	148
7.4	Conclusions	150
	References	151



## Chapter 8 Preparation and Characterization of Polyseudorotaxanes Based on Adamantane-Modified Polybenzoxazines and $\beta$ -Cyclodextrin

### Abstract

8.1	Introduction	166
8.2	Experimental	
8.2.1	Materials	168
8.2.2	Nuclear Magnetic Resonance (NMR)	168
8.2.3	Wide Angle X-ray Diffraction (WAXD)	168
8.2.4	Differential Scanning Calorimetry (DSC)	169
8.2.5	Thermogravimetric Analysis (TGA)	169

8.2.6 Synthesis of the $\beta$ -CD/ <u>2</u> benzoxazine inclusion complex	169
8.2.6 Synthesis of the $\beta$ -CD/ <u>3</u> benzoxazine inclusion complex	170
8.3 Results and Discussion	
8.3.1 Wide Angle X-ray Diffraction Analysis	171
8.3.2 Nuclear Magnetic Resonance Analysis	172
8.3.3 Proton $T_{1\rho}^H$ Relaxation Time Analysis	173
8.3.4 Glass Transition Temperature Analysis	174
8.3.4 Thermogravimetric Analyses	175
8.4 Conclusions	176
References	177
	
Chapter 9 Conclusions and Future Outlook	
List of Publications	191
Introduction to Author	193

## List of Tables

	<b>Pages</b>
Table 2-1. Electrical Resistivities of Metals	13
Table 2-2. Dielectric Constant of Some Low $k$ Polymer Materials	15
Table 2-3. Properties Required for New Intermetal Dielectrics	16
Table 2-4. Electronic Polarizability and Bond Enthalpies	18
Table 3-1. Curve fitting of fraction of hydrogen-bonding results of the PBZZ/PVP blends at room temperature	49
Table 3-2. IPP/CHEX data	49
Table 3-3. EPr/IPP/CHEX mixture-determination of $K_A$ and $K_A^{Std}$	50
Table 4-1. The Values of $m$ , $n$ , $k$ and Total Order of Different Curing Temperature	73
Table 5-1. The Dielectric Constant and Dissipation Factor of B-a/F-1 co-PBZZ at 298 K & $10^5$ Hz	99
Table 5- 2. The Weight Loss of B-a/F-1 co-PBZZ under $N_2$ Environment	99
Table 5-3. The Percentages of Water Absorption of B-a/F-1 co-PBZZ at Room Temperature	100
Table 6-1. Results of the Homopolymerization of $\epsilon$ -Caprolactone (CL) with Various Amounts of pa-OH in the Bulk at 120 °C and $[CL]/[Sn(Oct)_2] = 1000$ ; Polymerization Time: 24 h	129
Table 6-2. Curve fitting of fraction of hydrogen-bonding results of the pa-PCL/PBZZ copolymers at room temperature	129
Table 6-3. Glass transition temperatures, melting temperatures, and heats of melting	



of different pa-PCL/PBZZ composites	130
Table 7-1. The compositions and $T_g$ s of p-a/ <u>2</u> benzoxazine and p-m/ <u>3</u> benzoxazine co-PBZZs	154
Table 7-2. The weight loss and char yield of poly( <u>2</u> benzoxazine) and poly( <u>3</u> benzoxazine) under $N_2$ environment	154
Table 8-1. Weight losses temperatures, temperatures of maximum weight losses rates, and char yields of (a) $\beta$ -CD, (b) poly( $\beta$ -CD/ <u>2</u> benzoxazine IC) and (c) poly( $\beta$ -CD/ <u>3</u> benzoxazine IC ) under $N_2$ atmospheres	179



## List of Figures

	Pages
Figure 3-1. The DSC scans of PBZZ /PVP blends with different composition	53
Figure 3-2. $T_g$ versus composition curved base on PBZZ/PVP blends	54
Figure 3-3. FTIR spectra recorded at room temperature between $1620^{-1}$ - $1730\text{cm}^{-1}$	55
Figure 3-4. Infrared difference spectra of IPP/CHEX solutions recorded at room temperature	56
Figure 3-5. Infrared difference spectra of IPP/CHEX solutions with different IPP concentrations recorded at room temperature	57
Figure 3-6. Absorptivity coefficient of IPP in cyclohexane at room temperature	58
Figure 3-7. $K_2$ and $K_B$ of IPP in cyclohexane at room temperature	58
Figure 3-8. Infrared difference spectra of IPP/EPr/CHEX solutions recorded at room temperature	59
Figure 3-9. Infrared difference spectra of IPP/DMA/CHEX solutions recorded at room temperature	60
Figure 4-1. Dynamic DSC exothermic curves at different scan rates	75
Figure 4-2. Reaction rate versus isothermal curing time at different curing temperatures	76
Figure 4-3. Conversion versus isothermal curing time at different curing temperatures	77
Figure 4-4. The tendency of reaction rate versus conversion	78
Figure 4-5. Plots for determination of the activation energy of curing reaction by Kissinger method	79
Figure 4-6. Plots for determination of the activation energy of curing reaction by	

Flynn-Wall-Osawa method	80
Figure 4-7. Plots of $\ln k$ versus $1000/T$ for determination of the activation energy and Arrhenius preexponential of curing reaction by isothermal method	81
Figure 4-8. The DSC curves at different curing temperatures for 4hr	82
Figure 4-9. FTIR spectra recorded at room temperature between (a) 600-1600 $\text{cm}^{-1}$ (b) 2400-4000 $\text{cm}^{-1}$	83
Figure 5-1. The $^1\text{H}$ -NMR spectrum of F-1 benzoxazine	102
Figure 5-2. The $^{19}\text{F}$ -NMR spectra of (a) 4-(trifluoromethyl)aniline, (b) hexafluorobisphenol A	103
Figure 5-3. The $^{19}\text{F}$ -NMR spectrum of F-1 benzoxazine	104
Figure 5-4. The FT-IR spectrum of F-1 benzoxazine	105
Figure 5-5. The DSC scans of B-a/F-1 co-PBZZ copolymers with different composition	106
Figure 5-6. $T_g$ versus composition curved base on B-a/F-1 co-PBZZ copolymers	107
Figure 6-1. $^1\text{H}$ NMR spectra of pa-OH	131
Figure 6-2. $^1\text{H}$ NMR spectra of pa-PCL( $M_n=24000$ )	132
Figure 6-3. The FTIR spectra of (a) pa-PCL( $M_n=3000$ , 1a), (b) pa-PCL( $M_n=14800$ , 1b), (c) pa-PCL( $M_n=24000$ , 1c), (d) pa-PCL/PBZZ ( $M_n=3000$ , 2a), (e) pa-PCL/PBZZ ( $M_n=14800$ , 2b), (f) pa-PCL/PBZZ ( $M_n=24000$ , 2c) recorded at room temperature between 1680-1780 $\text{cm}^{-1}$	133
Figure 6-4. The FTIR spectra of (a) pa-PCL ( $M_n=3000$ , 1a), (b) pa-PCL/PBZZ ( $M_n=3000$ , 2a), (c) porous PBZZ ( $M_n=3000$ , 3a) recorded at room	

temperature between 1400 to 1800  $\text{cm}^{-1}$  134

Figure 6-5. The DSC scans of (a) pa-PCL( $M_n=3000$ , 1a), (b) pa-PCL( $M_n=14800$ , 1b), (c) pa-PCL( $M_n=24000$ , 1c), (d) pa-PCL/PBZZ ( $M_n=3000$ , 2a), (e) pa-PCL/PBZZ ( $M_n=14800$ , 2b), (f) pa-PCL/PBZZ ( $M_n=24000$ , 2c), (g) pure PBZZ ranging from (A) -120 to 0  $^{\circ}\text{C}$ , (B) 0 to 100  $^{\circ}\text{C}$ , and (C) 120 to 240  $^{\circ}\text{C}$  135

Figure 6-6. The TGA thermograms of (a) pa-PCL (b) pa-PCL/PBZZ (c) pa-PCL/PBZZ after hydrolysis, based on various molecular weights of pa-PCL 136

Figure 6-7. FE-SEM of cross-sectional images of pa-PCL/PBZZ copolymers at high magnifications (a) (3a, 50KX), (b) (3a, 100KX), (c) (3b, 50KX), (d) (3b, 100KX), (e) (3c, 50KX), (f) (3c, 100KX) 137

Figure 6-8. The dielectric constant of (a) different molecular weights pa-PCL at constant 25 wt % loading at  $10^5$  Hz and 298 K (b) different loading percentages of the pa-PCL ( $M_n=3000$ ) 139

Figure 7-1. The  $^1\text{H-NMR}$  spectrum of 4-(1-Adamantyl)phenol 155

Figure 7-2 The  $^1\text{H-NMR}$  spectrum of 2 benzoxazine 156

Figure 7-3. The  $^1\text{H-NMR}$  spectrum of 3 benzoxazine 157

Figure 7-4. The FT-IR spectra of (a) 2 benzoxazine and (b) poly(2 benzoxazine) 158

Figure 7-5. The FT-IR spectra of (a) 3 benzoxazine and (b) poly(3 benzoxazine) 159

Figure 7-6. The DSC scans of p-a type PBZZ, poly(2 benzoxazine), p-m type PBZZ, and poly(3 benzoxazine) 160

Figure 7-7. The DSC scans of p-a/2 benzoxazine co-PBZZ copolymers with different

composition	161
Figure 7-8. The DSC scans of p-m/3 benzoxazine co-PBZZ copolymers with different composition	162
Figure 7-9. Tg versus composition curved base on (a) p-m/3 benzoxazine and (b) p-a/2 benzoxazine PBZZs copolymers	163
Figure 7-10. The TGA thermogram of (a) p-m type PBZZ (b) p-a type PBZZ (c) poly(3 benzoxazine) (d) poly(2 benzoxazine) under N <sub>2</sub> environment	164
Figure 8-1. Powder X-ray diffraction patterns of (a) $\beta$ -CD, (b) <u>2</u> benzoxazine, (c) $\beta$ -CD/ <u>2</u> benzoxazine IC, and (d) poly( $\beta$ -CD/ <u>2</u> benzoxazine IC)	181
Figure 8-2 . Powder X-ray diffraction patterns for (a) $\beta$ -CD, (b) <u>3</u> benzoxazine, (c) $\beta$ -CD/ <u>3</u> benzoxazine IC, and (d) poly( $\beta$ -CD/ <u>3</u> benzoxazine IC)	182
Figure 8-3. <sup>13</sup> C CP/MAS NMR spectra of (a) $\beta$ -CD, (b) $\beta$ -CD/ <u>2</u> benzoxazine IC, and (c) $\beta$ -CD/ <u>3</u> benzoxazine IC	183
Figure 8-4. <sup>1</sup> H NMR spectra of (a) $\beta$ -CD, (b) $\beta$ -CD/ <u>2</u> benzoxazine IC, and (c) $\beta$ -CD/ <u>3</u> benzoxazine IC	184
Figure 8-5. Proton $T_{1\rho}^H$ relaxations of (a) $\beta$ -CD, (b) $\beta$ -CD/ <u>2</u> benzoxazine IC, and (c) $\beta$ -CD/ <u>3</u> benzoxazine IC	185
Figure 8-6. DSC scans of (a) poly( <u>2</u> benzoxazine), (b) poly( $\beta$ -CD/ <u>2</u> benzoxazine IC), (c) poly( <u>3</u> benzoxazine), (d) poly( $\beta$ -CD/ <u>3</u> benzoxazine IC)	186
Figure 8-7. (A) The TGA trace of (a) $\beta$ -CD, (b) poly( $\beta$ -CD/ <u>2</u> benzoxazine IC), and (c) poly( $\beta$ -CD/ <u>3</u> benzoxazine IC ). (B) Plots of derivative weight per degree C of (d) $\beta$ -CD, (e) poly( $\beta$ -CD/ <u>2</u> benzoxazine IC) and (f) poly( $\beta$ -CD/ <u>3</u> benzoxazine IC ) under N <sub>2</sub> atmospheres	187

## 摘要

於高分子的領域中，其化學性質與物理性質皆具有相當的重要性，且兩者亦是相輔相成。藉由化學改質的方法來滿足某些物理性質的需求、或是以物理性質研究來延續合成產物的應用性與實用性，而本論文主要是以改質高分子的功能性、強化實際使用的可行性、並針對這些新型高分子的物性與化性作一深切的討論。文中以 polybenzoxazine 為研究主體，內容則著重於以下所列之三大主題：

### (1) polybenzoxazine 與高分子間作用力以及熱交聯行為之研究

在分子的物理性質研究中，相容性(Miscibility)和特殊作用力(Specific Interaction)的探討，一直都是相當有趣的主题；且常有助於解釋許多的高分子行為。其中氫鍵作用力(Hydrogen bonding interaction)的探討更是本實驗室多年來研究的主要方向之一，本文研究之主體：polybenzoxazine 可產生氫鍵予體，並可與其它氫鍵受體的高分子產生氫鍵作用力，使得混摻高分子的諸多性質因而大大提昇。再者，藉由對其熱交聯行為深入的研究，將有助吾人控制 polybenzoxazine 各種性質的優與劣，並能徹底瞭解此一新型高分子的各項特性。

### (2) polybenzoxazine 於低介電材料之研究

低介電材料一般主要是作為絕緣材料用，它的研究伴隨著積體電路(IC)線寬的縮小日形重要，介電值已由傳統 4 左右的  $\text{SiO}_2$  逐步進展到了 3 以

下，甚至許多的研究已經達到 2 以下的水準，時至今日，介電值小於 3 的材料才真正具有較大的應用性。在不改變現行銅製程的情況下，選用低介電值之材料作為絕緣用，乃是大幅地降低  $RC$  delay 影響的最直接方法，這也是為何低介電材料被如此廣泛的研究與討論。而 polybenzoxazine 本身具有一些相當優異的性質，如：交聯後的收縮率趨近於零、熱安定性高、低吸水性、高玻璃轉移溫度…等等，此外，有別於一般高單價的低介電材料，polybenzoxazine 具有相當的成本優勢。吾人以 polybenzoxazine 作為低介電材料的基材，並利用(a)氟化此高分子與(b)製成奈米級的多孔性材料的方法，來降低 polybenzoxazine 的介電值，並開展出 polybenzoxazine 的另一種新用途。



### (3) 金剛烷修飾之 polybenzoxazine 與環糊精錯合的基礎研究

本文同時將一個立體阻礙較大的環狀取代基(金剛烷：adamantane)；鍵結到 polybenzoxazine 的高分子鏈上，以提昇此高分子的玻璃轉移溫度。再者，吾人利用金剛烷可和  $\beta$ -環糊精( $\beta$ -cyclodextrin)形成錯合(complex)的特性，使得經金剛烷修飾後的 polybenzoxazine 與  $\beta$ -環糊精形成具有特殊的晶體結構，並利用廣角 X-ray 散射、 $^1\text{H}$  液態核磁共振儀與  $^{13}\text{C}$  CP/MAS 固態核磁共振儀來鑑定與探討此一結構與型態，並深入研究此一結構對各種性質所造成之影響。

## Abstract

The physical properties and chemical properties are both important in the polymer researches. Many properties will be enhanced after modifying the polymers. In this thesis, we focus on three major subjects which based on the polybenzoxazines:

### **(1) The studies of polymer interaction and thermal curing behavior of polybenzoxazines**

We concentrate on the polymer miscibility and specific interaction, especially in the hydrogen bonding interaction. The polybenzoxazine contains hydroxyl group that is known as a proton donor for several polymers with proton acceptor, and many properties were enhanced after inducing the hydrogen bonding interaction. Furthermore, we could control and understand the properties of polybenzoxazines by studying its thermal curing behavior.

### **(2) The studies of polybenzoxazine in low dielectric materials**

Low dielectric constant materials ( $k < 3.0$ ) have the advantage of facilitating manufacture of higher performance integrated-circuit (IC) devices with decreasing feature size of the chip. After replacing the aluminum process by the copper process, the most feasible approach is to use an insulating material possessing a lower dielectric constant without changing the copper process. Polybenzoxazine resins were found to possess several outstanding properties that fit the requirements of low dielectric constant materials, such as near-zero shrinkage after curing, high thermal stability, low water absorption, high glass transition temperature and low price. In the section, we used two methods including fluorinating polybenzoxazine and forming porous structures in the course of developing low dielectric constant materials.



### **(3) The studies of polyseudorotaxanes based on adamantane-modified polybenzoxazines and cyclodextrin**

In general, a polymer containing a cyclic alkyl substitute tends to raise its  $T_g$ . In addition, positioning the mass center of the substitute closer to the polymer backbone will increase the bulkiness of the substitute and thus become more effective for  $T_g$  increasing. In the section, we incorporated adamantane as a pendant group into the polybenzoxazine structure and enhanced its thermal properties. Furthermore, the pendant group, adamantane, forms stoichiometric complexes with  $\beta$ -cyclodextrin ( $\beta$ -CD) and fine crystalline powders are obtained. We characterized these complexes by powder X-ray diffraction,  $^1\text{H}$  NMR spectroscopy,  $^{13}\text{C}$  and  $^{13}\text{C}$  CP/MAS NMR spectroscopies. A detail discussion was made in order to analyze the effect that caused by the crystalline complex structure.

